

Excited-State Planarization as Free Barrierless Motion in a π -Conjugated TerpyridineRonald Siebert,[†] Andreas Winter,[‡] Ulrich S. Schubert,^{*,§} Benjamin Dietzek,^{*,†,||} and Jürgen Popp^{†,||}

Institute of Physical Chemistry, Friedrich-Schiller-University Jena, Helmholtzweg 4, 07743 Jena, Germany, Laboratory of Macromolecular Chemistry and Nanoscience, Eindhoven University of Technology, P.O. Box 513, 5600 MB Eindhoven, The Netherlands, Laboratory of Organic and Macromolecular Chemistry, Friedrich-Schiller-University Jena, Humboldtstr. 10, 07743 Jena, Germany, and Institute of Photonic Technology, Albert-Einstein-Str. 9, 07745 Jena, Germany

Received: January 12, 2010; Revised Manuscript Received: February 24, 2010

We present femtosecond time-resolved transient absorption data and results from nanosecond time-resolved emission studies for an extended terpyridine system (4'-((2,5-bis(octyloxy)-4-styrylphenyl)ethynyl)phenyl)-2,2':6',2''-terpyridine). By variation of selected solvent properties, that is, solvent viscosity, polarity, and temperature, we can dissect kinetic components, which are due to photoinduced molecular structure rearrangements of the terpyridine system. This real-time observation allows us to quantify the influence of the solvent viscosity on the structural rearrangements, which becomes slowed from 20 to 100 ps when changing the solvent from methanol to *n*-butanol. By adding temperature-dependent time-resolved emission experiments to the study, we show that the relaxed S₁ state partially decays via a nonradiative channel which can be assigned to an intersystem crossing to a lower lying T₁ state. The data presented in this paper directly visualize excited-state planarization of the terpyridine sphere in real time. Such motion of the terpyridine with respect to the adjacent conjugated rest leads to a highly conjugated chromophore and is causative for the observed photophysical features of the ligands and their transition metal complexes.

Introduction

The conversion of light into chemical and electrical energy by means of artificial photosynthesis¹ and organic solar cells with properties tailored on the molecular level² represents a major challenge in modern chemistry. One of the key steps in harvesting and conversion of sun light, which will greatly help dealing with the looming energy crisis,^{1b} is efficient light harvesting by mimicking natural photosynthesis or in photovoltaic applications. There are several approaches to this problem using different strategies like supramolecular frameworks,³ organic semiconductors,⁴ or metal-organic polymers, in which photoactive transition-metal centers are connected by different photoactive bridging ligands.^{2b,5} The design of such systems allows for spectral-spatial focusing of the absorbed photon energy to a reaction center or photoactive electron donor.

Generally, transition metal complexes of 2,2':6',2''-terpyridine ligands,⁶ for example, [Ru(tpy)₂]²⁺, exhibit less useful photophysical properties than their 2,2'-bipyridine-based counterparts in terms of application for luminescent devices.⁷ However, they are structurally more appealing with respect to the realization of linear assemblies, for example, as molecular wires.⁸ Therefore, much effort has been laid on the design and synthesis of terpyridine-based ligands and their transition metal complexes with enhanced photophysical properties.^{7a,9} Approaches incorporating electron-withdrawing and electron-donating substitu-

ents,¹⁰ replacing the external pyridines by other heterocyclic rings¹¹ and extending the π -conjugated system¹² have recently been discussed.

The approach followed here is to adopt the major structural features of the most common poly(phenylene-ethynylene)-*alt*-poly(phenylene-vinylene)-type polymers¹³ and to connect them to phenyl-substituted terpyridine spheres, which can subsequently be coordinated to transition-metal centers.¹⁴ Such systems are well-known to stabilize MLCT states in the resultant transition-metal complexes due to delocalization of the MLCT over the entire chromophore.^{7a} A substantial prerequisite for the success of this approach is the introduction of sufficient conjugation between the terpyridine-unit and the conjugated substituent. In this context it was shown that the conjugation between the two molecular parts is perturbed by the torsion of the terpyridine-plane with respect to the chromophore and has a strong influence on the photophysical properties of the ligand systems and their metal complexes.¹⁵

To evaluate the light-harvesting properties of such terpyridine-based supramolecular systems in real time, femtosecond time-resolved spectroscopy is applied. We previously focused on investigating the photophysics of related terpyridine-based ligand systems, which consist of one up to four terpyridine spheres connected by a π -conjugated spacer.¹⁶ These ligands will form the structural basis for building one- or two-dimensional metallo-organic polymers for potential light-harvesting applications and operation in organic light-emitting diodes. We have investigated their photophysical properties, which are expected to have strong influence on the spectroscopic features of supramolecular architectures based terpyridine coordination polymers. These first experiments showed the formation of an emissive molecular geometry within picoseconds, which decays on a ns time-scale into a long-lived nonemissive triplet state.

* To whom correspondence should be addressed. Phone: 0049-3641-206332. Fax: 0049-3641-206399. E-mail: benjamin.dietzek@uni-jena.de.

[†] Institute of Physical Chemistry, Friedrich-Schiller-University Jena.

[‡] Eindhoven University of Technology.

[§] Laboratory of Organic and Macromolecular Chemistry, Friedrich-Schiller-University Jena.

^{||} Institute of Photonic Technology.

Here, we focus on solvent-dependent time-resolved experiments to obtain substantially more insight into the photoinduced excited-state processes in the structurally most simple terpyridine system 4'-((4-((2,5-bis(octyloxy)-4-styrylphenyl)ethynyl)phenyl)-2,2':6',2''-terpyridine, consisting of a conjugated backbone and one terpyridine sphere (abbreviated "monoterpyridine" in the following). The experiments presented aim at discriminating between ultrafast intramolecular charge-transfer dynamics from excited-state structural rearrangements. The latter process has been discussed extensively in the literature on conjugated terpyridine systems in the context of excited-state planarization, which enlarges the π -electron system and stabilizes the excited state by stronger conjugation. However, the importance of such excited-state planarization has been inferred from the luminescence properties of synthetically modified terpyridine systems, and transient absorption experiments on terpyridine metal complexes.¹⁷ In these cases the importance of this motion as a gating process was realized. The study at hand aims at a detailed femtosecond time-resolved investigation of the photoinduced planarization in isolated terpyridine model systems, in particular with respect to the solvent dependence of this reaction. The formation of an intramolecular charge-transfer state, the spectroscopic properties of which strongly vary with solvent polarity takes place in several small conjugated systems such carbonyl-substituted polyenes¹⁸ as well as in, for example, carbonyl-substituted chlorophyll-derivates.¹⁹ To disentangle intramolecular charge-transfer (ICT) from excited-state structural rearrangements and from other possible ultrafast relaxation processes, the solvent properties are systematically varied here. Variation of the solvent viscosity will affect any process associated with large structural rearrangement due to the local friction asserted on the solute by the solvent cage, the stiffness of which is correlated with the solvent viscosity.

A detailed and in-depth knowledge about these processes and their manifestation within the excited-state relaxation pathway in terpyridine based systems such as monoterpyridine will provide the basic framework for the synthesis of organo-metallic polymers and complexes with tailored electro-optical properties.

Experimental Section

The synthesis of the series of π -conjugated terpyridine was recently published elsewhere.²⁰ The time-resolved transient absorption setup, which was described previously,¹⁶ is based on an amplified Ti:Sapphire oscillator (Libra, Coherent Inc.) producing a pulse-train of 80 fs 950 μ J pulses centered at 800 nm with a repetition rate of 1 kHz. The pulses were split by means of a 50:50 beamsplitter. One pulse-train was used to pump a noncollinear optical-parametric amplifier (TOPASwhite, LightConversion Ltd.), while the other one generated the pump pulses by second harmonic generation a 100 μ m thick BBO crystal. In some experiments reported here, white light was used as probe. Therefore, 1% of the 800 nm fundamental beam was split off and focused into a sapphire plate to generate a supercontinuum.

It was ensured that the energy of the pump pulses was kept well below 0.5 μ J, while typical probe intensities fall into the range of a few hundred nJ. Autocorrelation of the probe pulses and the experimental response function were recorded at the sample position by noncollinear second harmonic generation in a BBO crystal. The temporal duration of the probe pulses and the experimental response function was estimated to be in the order of 50–60 fs. Steady-state absorption spectra were frequently recorded to monitor the sample integrity.

Fluorescence lifetimes were obtained by time-correlated single-photon counting. Therefore, a Ti:Sapphire Laser (Tsu-

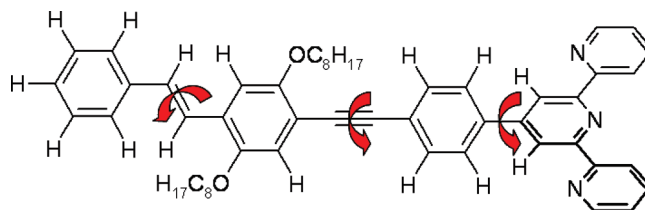


Figure 1. Schematic representation of the molecular structure of the investigated monoterpyridine.

nami, Newport Spectra-Physics GmbH) was used as light source. The repetition rate was reduced to 800 kHz by a pulse selector (Model 3980, Newport Spectra-Physics GmbH) and afterward the beam was frequency doubled in a second harmonic generator (Newport Spectra-Physics GmbH) to create the 435 nm pump beam. The emission was detected using a Becker & Hickel PMC-100-4 photon-counting module with 150 ps response-limited time resolution. To control the temperature of the sample an Oxford Instruments ITC 503 intelligent temperature monitor and control unit was used.

Steady-state absorption spectra were recorded on a Jasco V-670 spectrophotometer, the fluorescence spectra were measured from dilute solutions using a Jasco FP-6200 spectrofluorimeter. All used solvents were of spectroscopic grade and purchased from Merck or Sigma Aldrich. The samples were prepared to yield an optical density of 0.1 in a 1 mm quartz-glass cuvette at the long wavelength absorption maximum.

Results and Discussion

Steady-State Spectroscopy. Figure 2a shows the absorption and emission spectra of the *tpy* system dissolved in acetonitrile and toluene. These solvents represent the vertices of a number of binary mixtures of these highly polar and nonpolar solvents, which were used to investigate the effect of solvent polarity on the steady-state absorption and emission properties of the sample (Table 1).

Figure 2a shows that the spectral properties of the monoterpyridine strongly depend on the solvent polarity. This is reflected by the different shapes of the emission spectra when dissolving the sample in toluene and acetonitrile, respectively. The two main effects are a red shift of the emission maximum upon dissolution in the polar solvent and a loss of vibrational structure in the fluorescence spectrum, while the effect on the absorption spectra is weaker (see Figure 2). The qualitative solvent dependence becomes more quantitative in Figure 2b. Steady state spectra in different solvent environments with increasing polarity unravel the effect of polarity on the electronic transitions. To recover values for the Stokes shift as a function of solvent polarity, both absorption and emission spectra were deconvolved into two (absorption) and three (emission) Gaussian profiles to account for the vibrational structure (see the Supporting Information and ref 16 for details). From the deconvolved data, the Stokes shift was determined and plotted as a function of the solvent polarity, which was determined according to eq 1 [Equation 1: Polarity of the solvent (Δf), calculated from the static dielectric constant (ϵ) and the refractive index (n).] Linear regression of the data was carried out using the Lippert eq 2.²¹ [Equation 2: Dependence of the Stokes shift ($\nu_{\text{abs}} - \nu_{\text{em}}$) from the solvent polarity, the difference in excited-state and ground-state dipole moment ($\mu_e - \mu_g$), and the radius of the solvent cage (a).]

$$\Delta f = \frac{\varepsilon - 1}{2\varepsilon + 1} - \frac{n^2 - 1}{2n^2 + 1} \quad (1)$$

$$v_{\text{abs}} - v_{\text{em}} = \frac{2}{hc} \left(\frac{\varepsilon - 1}{2\varepsilon + 1} - \frac{n^2 - 1}{2n^2 + 1} \right) \frac{(\mu_e - \mu_g)^2}{a^3} \quad (2)$$

Both the Stokes shift and the emission lifetime reveal a linear increase with increasing solvent polarity. This finding can be understood when invoking a higher dipole moment of the first excited state with respect to the electronic ground state. Such an excited state will be energetically more stabilized in polar environments compared to the electronic ground state. Hence, in more polar solvents, both the Stokes shift and the emission lifetime will increase. The linear dependences of Stokes shift and emission lifetime in concert with the minor effect of polarity on the absorption spectra indicate that absorption and emission involve the ground and the first excited state only: they occur between the electronic ground state and a $\pi\pi^*$ excited state without the contribution of a charge-transfer state.²² It should be mentioned that the excitation is localized on the entire π -system and not only on the conjugated substituent of the terpyridine sphere, as corroborated by DFT calculations and Raman experiments on related systems.¹⁵

Ultrafast Picosecond Photoinduced Dynamics. The steady-state absorption and emission spectra as a function of solvent polarity reveal the nature of the electronic transitions observed. However, they do not yield direct insight into excited-state equilibration processes, which will take place upon photoexcitation. In order to monitor the dependence of such ultrafast processes on the molecular environment, we performed femtosecond time-resolved transient absorption experiments. Such experiments are presented and discussed in the following. In doing so, we aim at disentangling the effect of solvent polarity and solvent viscosity on the ultrafast, that is, sub-100-ps photoinduced dynamics of the tpy system. For the sake of clarity,

TABLE 1: Comparison of the Data from the Solvent-Dependent Measurements^a

solvent vol % toluene in acetonitrile	Δf	ν_1/cm^{-1}	ν_2/cm^{-1}	$\Delta\nu/\text{cm}^{-1}$
0	0.71	24741	22609	2133
10	0.64	24682	22621	2061
20	0.57	24591	22644	1947
30	0.50	24621	22631	1990
40	0.43	24596	22664	1932
50	0.36	24642	22687	1955
60	0.29	24564	22722	1842
70	0.22	24571	22765	1806
80	0.15	24565	22817	1748
90	0.08	24587	22903	1,683
100	0.01	24597	23,050	1547
methanol	0.71	25018	22772	2245
acetone	0.65	24816	22744	2072
THF	0.44	24716	22754	1962

^a Column one represents the solvent mixtures from toluene and acetonitrile or the pure solvents, f refers to the polarity of the solvent system, and ν_1 and ν_2 are the maxima of the deconvolved absorption and emission spectra, respectively.

we will present the results of polarity and viscosity-dependent transient-absorption experiments separately before suggesting an overall explanation for the observed behavior.

Solvent-Polarity Dependence. The formation of an intramolecular charge-transfer state upon photoexcitation has been discussed in the literature for terpyridines and terpyridine-related systems, in particular for their zinc(II) complexes.^{12,14b,23} Furthermore, it is a common feature in other strongly conjugated systems such as carbonyl-substituted carotenoids¹⁸ and chlorophyll derivatives.¹⁹ Commonly, all these systems exhibit a strongly solvent-polarity dependent excited-state behavior,^{18b,24} which is indicative of an ICT state. This solvent-polarity dependence stems from the enlarged excited-state molecular dipole upon formation of an ICT state that is consequently more stabilized in polar solvents compared to nonpolar ones. Hence, ICT

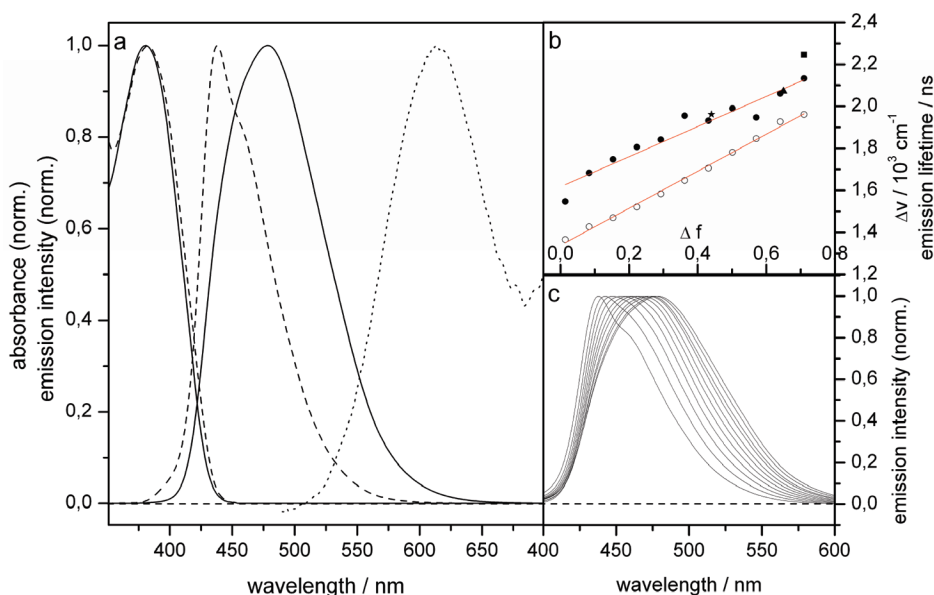


Figure 2. (a) Comparison of the absorption and emission spectra of the analyte using toluene (dashed line) and acetonitrile (solid line) as solvent with a transient absorption spectra at 500 ps recorded in THF (dotted line). (b) Polarity dependence of the Stokes shift in 10^3 cm^{-1} (solid circles represent binary mixtures of toluene and acetonitrile, while the square/triangle/star refers to methanol/THF/acetone as solvent, respectively) and the emission lifetime in ns (open circles). The red lines are the linear regression to the data points. (c) Comparison of the emission spectra recorded in the different binary mixtures. Here, it can be noted that the vibrational structure of the spectrum vanished, when the solvent polarity is gradually changed from nonpolar to highly polar.

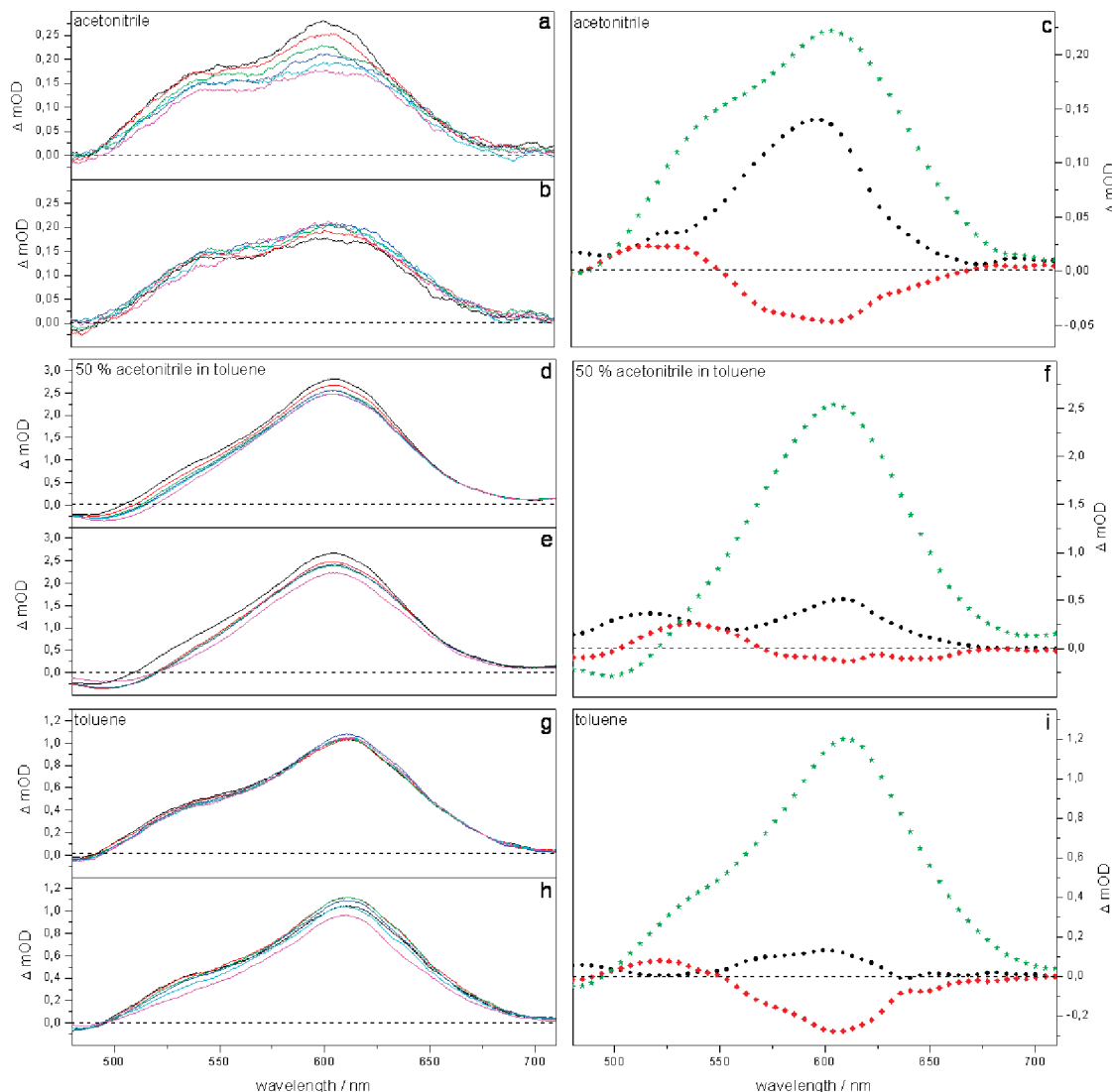


Figure 3. Transient-absorption spectra for the tpy dissolved in three solvents of different toluene content in acetonitrile (0% $\Delta f = 0.71$; 50% $\Delta f = 0.36$; 100% $\Delta f = 0.01$). Panels a, d, and g compare transient spectra between 0 and 10 ps after excitation (0.5 ps black; 1.0 ps red; 2.5 ps green; 5.0 ps blue; 7.5 ps cyan; and 10.0 ps magenta), while panels b, e, and h show transient spectra between 10 and 500 ps (10 ps black; 25 ps red; 50 ps green; 100 ps blue; 250 ps cyan; and 500 ps magenta). Panels c, f, and i depict the respective decay-associated spectra for a three-exponential decay with 2.0–3.0 ps (black squares), 15–20 ps (red circles), and a nanosecond component (green stars). Due to the limited delay-time range accessible in our experimental arrangement, a precise estimate of this time constant based on transient-absorption data is not possible. However, the results from time-resolved emission experiments allow us to provide more precise estimates (see ref 28).

formation will contribute to the transient-absorption kinetics with a strongly solvent-dependent component. To interrogate the system at hand with respect to the presence of an ICT state, transient-absorption experiments employing a supercontinuum white-light probe were carried out in different solvents, that is, toluene, acetonitrile, and a 50:50 mixture of both solvents (see Figure 3).

Figure 3a,b depicts transient-absorption spectra at different delay times for the monoterpyridine in acetonitrile, and panel c shows the decay-associated spectra, obtained from a triexponential global fitting procedure. Panels d–i show respective information for the monoterpyridine dissolved in toluene and the toluene–acetonitrile mixture. For all three solvent systems similar general decay behaviors are observed: Directly after photoexcitation the signal decays during the first 10 ps. This process is followed by a slower decay in the blue part and a rise of the signal in the red part of the transient spectra which is completed after roughly 250 ps. Finally, a slow overall decay of the signal is observed, which extends over the experimentally accessible delay-time window. The amplitudes of the first two

components relative to the slow component are larger for pure acetonitrile when compared to the other two solvent conditions. The decay in the blue and the rise in the red part of the spectrum on the intermediate time scale occur concertedly. A more quantitative description of the observed photophysics stems from a global fitting analysis, which resulted in three time-constants $\tau_1 = 2\text{--}3$ ps, $\tau_2 = 15\text{--}20$ ps, and $\tau_3 \approx \text{ns}$. The corresponding decay-associated spectra are shown in panels c, f, and i. Considering the decay-associated spectra the spectral features associated with the kinetic components are discussed. It can be seen, that the fast component causes an overall decay of the signal, followed by a slower component, which corresponds to a rise between 550 and 750 nm and a decay below 500 nm. The third exponent again represents an overall decay on a long time scale. Furthermore, it is obvious that the spectral distribution of the exponentials is rather equal for all solvents, representing systems with a very high, medium and very low polarity. Finally, it should be noticed that the data obtained from monoterpyridine in several solvent mixtures correlate well with data from previous studies, which were restricted to an

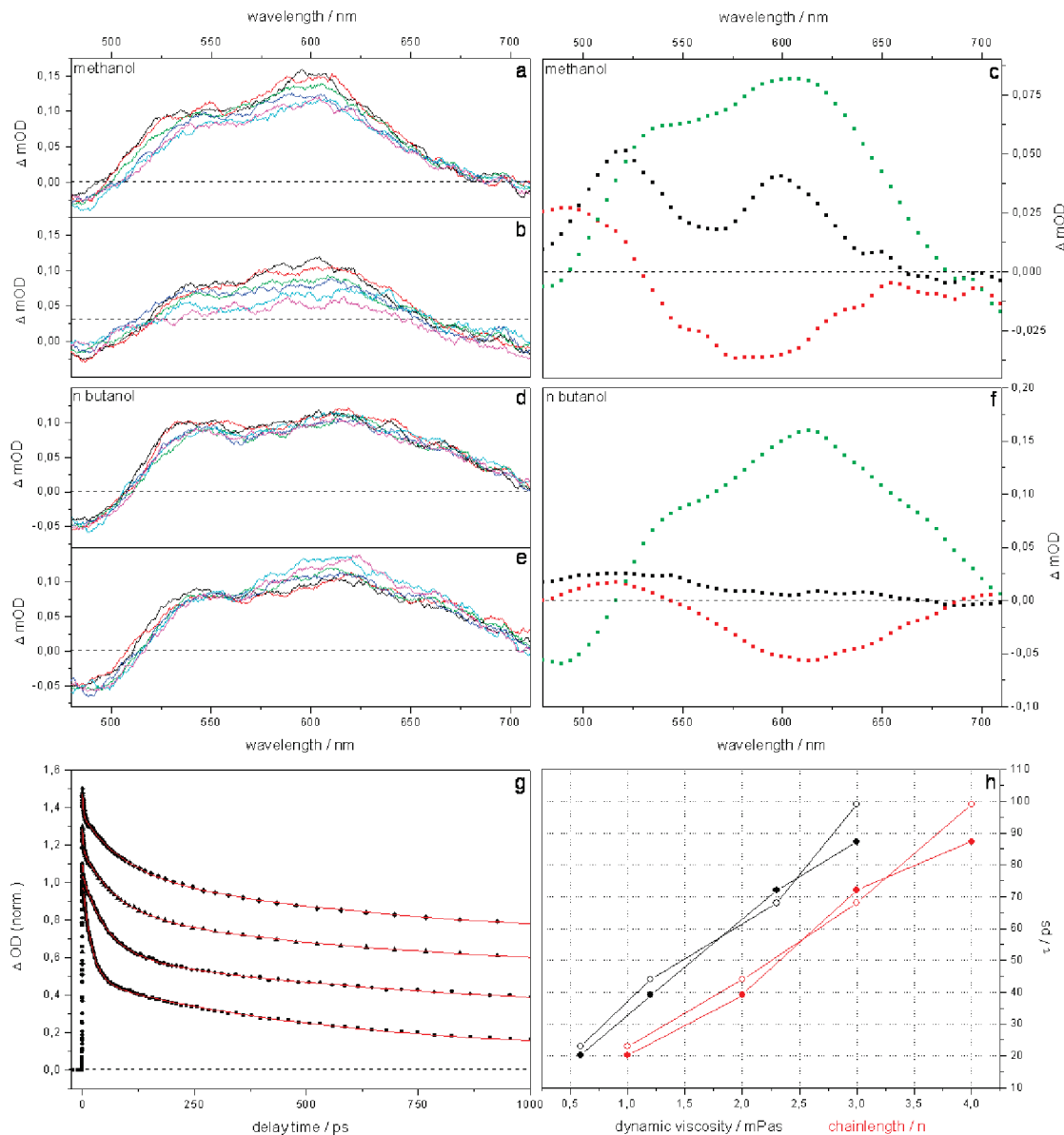


Figure 4. Transient-absorption spectra of monoterpyridine dissolved in methanol ($\Delta f = 0.71$) and *n*-butanol ($\Delta f = 0.61$). Panels a and d compare transient spectra between 0 and 10 ps after excitations (0.5 ps black; 1.0 ps red; 2.5 ps green; 5.0 ps blue; 7.5 ps cyan; and 10.0 ps magenta), while panels b and e show transient spectra between 10 and 500 ps (10 ps black; 25 ps red; 50 ps green; 100 ps blue; 250 ps cyan; and 500 ps magenta). Panels c and f depict the respective decay associated spectra for a three exponential decay with 2.0–3.0 ps (black squares), 20–100 ps (red circles), and a nanosecond component (green stars). Figure 4g compares single kinetic traces recorded at 550 nm for methanol (squares), ethanol (circles), *n*-propanol (triangles), and *n*-butanol (diamonds) together with the respective triexponential fit (red line). Figure 4h shows the medium time constant (τ_2) as function of solvent viscosity (black) and the chain length of the alcohols (red). Full symbols represent data using single 550 nm as probe beam and the empty ones white light, respectively.

investigation of the photophysics of monoterpyridine in tetrahydrofuran.¹⁶

Thus, the solvent dependent transient-absorption data using a supercontinuum probe reveal no strong influence of the solvent polarity on the shape of the excited-state absorption spectra in the spectral observation window. This finding strongly indicates that the photophysics of monoterpyridine does not involve the formation of an ICT state. As spelled out before, in the latter case, we would expect strongly solvent polarity dependent spectral features.

Solvent-Viscosity Dependence. Aside from the formation of an ICT state, significant rearrangements of the molecular geometry in the excited electronic state of conjugated terpyridines have been discussed.^{7a,9} Photoinduced structural rearrangements as well as conceptually related isomerization

reactions²⁵ reveal a strong dependence on the solvent viscosity due to the interaction of the molecule with the surrounding solvent cage during the molecular motion.²⁶ Thus, recording differential absorption spectra as a function of solvent viscosity will help to distinguish ultrafast structural rearrangements from other photochemical or photophysical processes, because the kinetic components associated with severe geometrical changes of the solute are supposed to be slowed in the more viscous solvents.²⁷ To test if photoinduced structural rearrangements on the excited-state potential-energy surface are of significance for the terpyridine system, the tpy was dissolved in a series of *n*-alcohols ($n = 1-4$) and transient-absorption spectra as well as single wavelength kinetics were recorded.

Figure 4 compares the transient-absorption spectra for the monoterpyridine dissolved in the two alcohols methanol and

n-butanol. Panels a and b (d and e for butanol) depict transient-absorption spectra at different delay times, while panel c (f) shows decay-associated spectra, obtained from a triexponential global fit. Figure 3g compares single wavelength pump–probe kinetics recorded at 550 nm for methanol, ethanol, propanol, and butanol, while panel h summarizes the dependence of the time constant τ_2 on solvent viscosity and alcohol chain length. For all alcohols the general decay behavior is similar (Figure 3a, b, d, e, and h) and comparable to the data observed when using acetonitrile and toluene as solvents: A fast sub-10 ps signal decay is followed by a slower decay in the blue part and a rise of the signal in the red part of the transient spectra. Subsequently, an overall decay of the differential absorption signal is observed, which extends over the rest of the experimentally accessible delay-time window. While the fast process can be characterized with a time constant $\tau_1 = 2\text{--}3$ ps, irrespective of the solvent viscosity, the second process (τ_2) shows a drastic solvent viscosity dependence, yielding $\tau_2 = 20$ and 100 ps for methanol and butanol, respectively. To separately illustrate this behavior, Figure 4g compares single-wavelength kinetics recorded at 550 nm for the various alcohols. From these high S/N data, it is possible to determine precise values for the solvent-dependent characteristic time constants, which for τ_2 are summarized in Figure 4h. Figure 4h summarizes the solvent-dependence of τ_2 obtained from fitting the data shown in Figure 4. As can be seen, linear dependences of τ_2 on both solvent viscosity and alcohol chain length are observed.

The pronounced deceleration of the kinetic associated with τ_2 can be understood invoking a distinct change of the excited-state molecular geometry being associated with this component. Such an assignment is consistent with a number of publications, where strongly viscosity dependent time constants associated with isomerization reactions in solution have been reported.^{25,26,27a,28} This being stated, the question arises if the molecular bond can be identified, at which structural rearrangement dominantly takes place. Inspection of the molecular structure (see Figure 1) reveals three positions, where steric interactions and repulsion of substituents cause a distorted, that is, nonplanar, geometry. Hence, a weakened double-bond character in the excited-state of the conjugated chromophore offers the possibility for photoinduced torsional relaxation. One of these positions is the PPV-related part of the molecule. Here, the planar geometry is disturbed by the large octyloxy substituents. From *p*-phenylene-vinylene trimer, used as model compounds for PPV polymers, it is known that excited state planarization occurs directly after photoexcitation on a time scale in the order of 10 ps.²⁹ A second position, at which changes in the molecular structure are possible, is the ethynylene part. At this position excited-state planarization was also reported for PPE derivatives.³⁰ Furthermore, the terpyridine sphere is twisted roughly 35° away from the almost planar conjugated backbone. Theoretical approaches to determine the molecular structure in the electronic ground state, however, showed that the part with the most disturbed geometry is the terpyridine part, while the other substructures show only minor deviations from the planar conformation. (The ground state geometry was determined by DFT calculations and their comparison to the corresponding Raman and IR-spectra.) Therefore, it appears most plausible to assign the photoinduced structural changes to the orientation of the terpyridine sphere, which is twisted by roughly 35° with respect to the rest of the chromophore. In some terpyridine–metal complexes, such motions could be identified as a gating process in the relaxation pathway, which occurs on a sub 10 ps time scale. These considerations further hint to excited-state planarization being re-

sponsible for the herein observed ultrafast solvent-viscosity dependent photophysics of the monoterpyridine.¹⁷ The longer time scale for this process, observed in our experiments would be due to a more extended chromophore in this case, which causes a higher steric impact.

As a result of the twisted ground-state geometry, which is estimated based on DFT calculations on structurally related systems, the conjugation between the two parts of the molecular structure is decreased from its optimal value, that is, corresponding to the planar structure.¹⁵ Nonetheless, molecular torsion in the electronic ground state is not severe enough to electronically decouple both parts of the molecule, which still act as a single chromophore. Photoinduced torsional motion, however, should result in drastically altered spectral properties of the tpy system: A reduction of the torsion angle would increase the conjugation, while an increase of the torsion angle shall lead to a broken conjugation on the time scale of the torsional motion. These expectations are corroborated by the experimental results, because the data show signal decay in the blue part and a rising differential absorption band in the red with the characteristic time constant τ_2 . As indicated before, this observation can be explained by excited-state planarization: A distorted, blue absorbing chromophore, the geometrical structure of which resembles the ground-state structure, is converted into a planar, red absorbing chromophore by torsional relaxation. The excited-state potential-energy surface along this reaction coordinate seems to be rather flat as indicated by the almost linear dependence of the characteristic time constant τ_2 on the solvent viscosity (η)²⁶ and the local friction asserted by the solvent, which is reflected in the chain-length dependence of τ_2 .^{28a} Such linear behavior of the reaction rate has been previously observed in isomerization reactions and indicates that the respective molecular process occurs barrierless.^{25,28b}

Ultrafast Photoinduced Processes. The ultrafast sub-100-ps light-induced processes in the conjugated monoterpyridine derivative are dominated by two distinct time constants: $\tau_1 \approx 2.5$ ps and $\tau_2 = 20\text{--}100$ ps. While τ_1 is unaffected by either solvent viscosity or polarity, the kinetic process associated with τ_2 is slowed significantly in more viscous solvents. In agreement with previous work, the 2 ps component is assigned to cooling,³¹ which is known to occur on similar time scales. The subsequent viscosity dependent ps-component (τ_2) is assigned to excited-state planarization of the twisted terpyridine sphere, leading to a relaxed S_1 state. An overall red-shift of the S_1 excited-state absorption, which is independent of solvent polarity, is apparent from the spectral dependence of the τ_2 -associated amplitude. This finding indicates that τ_2 is not associated with intramolecular charge transfer. Thus, we conclude that photoinduced excited-state planarization of the conjugated terpyridine system takes place after photoexcitation on a picosecond time scale, a process that has been predicted to dominate the photochemistry of such dyes.^{9,32}

Nanosecond Fluorescence Dynamics. Having discussed the ultrafast formation of the emissive geometry above, the remainder of the paper will focus on the nanosecond fluorescence dynamics as observed in time-correlated single-photon counting experiments. In previous work, a nanosecond kinetic component was observed, which led to a decay of the fluorescence while populating a long-lived nonemissive triplet state.¹⁶ To obtain a more detailed insight in the solvent dependence of this process, temperature-dependent experiments have been conducted. To do so, emission lifetimes of the monoterpyridine in tetrahydrofuran (THF) were recorded as a function of temperature in the range between 300 and 170 K.

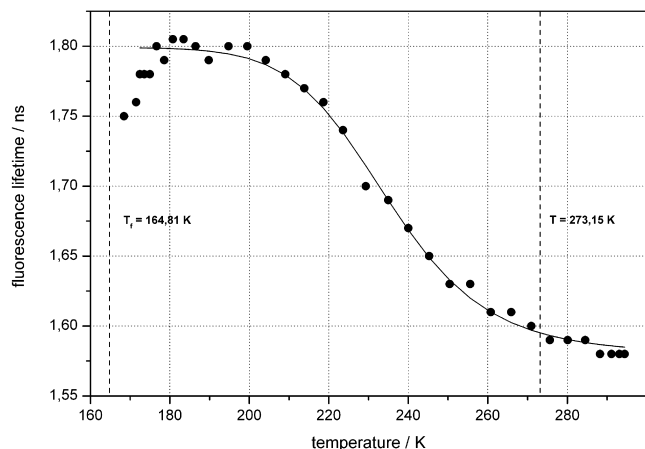


Figure 5. Temperature dependence of the emission lifetime of the monoterpyridine in THF. Symbols represent experimental data, while the solid line refers to the result of a fit. The vertical dashed lines indicate the fusion points of THF (164.8 K) and water (273.1 K), respectively.

Figure 5 summarizes the results of such experiments: At 300 K the emission lifetime is 1.58 ns. Reduction of the temperature below 290 K leads to an increase of the emission lifetime. The lifetime reaches its maximum values of roughly 1.80 ns at 180 K and decreases again slightly to 1.75 ns, when the temperature approaches the freezing point of THF at 164.8 K. Over the entire temperature range, the emission shows a monoexponential decay, the temperature dependence of which is typical for the presence of an excited-state barrier, dividing a radiative state and a nonradiative state. Monoexponential decay curves are recorded irrespective of the temperature, that is, no emission from T_1 is observed.

$$\tau(T) = \left[\frac{1}{\sum k + A \exp(-E_a/RT)} \right] + C \quad (3)$$

Before estimating the barrier-height from the temperature-dependent data, we shall refer to experiments attempting to induce a similar barrier for the depopulation of the emissive state by variations of the macroscopic solvent viscosity at room temperature. Such experiments were performed by dissolution of monoterpyridine in a series of *n*-alcohols or in mixtures of acetone and acetylcellulose (see Supporting Information for details). While adding acetylcellulose to acetone causes a drastic increase in viscosity, no effect on the emission lifetime could be observed. On the other hand, dissolution of the tpy in a series of *n*-alcohols causes only a slight decrease in the lifetime with increasing chain length, an effect that is assigned to the decreasing polarity of higher alcohols. This result indicates that quenching of the fluorescence does not involve major structural rearrangements of the molecular structure. The nonradiative decay of the long-lived species occurs by internal conversion (IC) or intersystem crossing (ISC) and does not alter the molecular geometry, while both processes compete with each other at room temperature. However, the nonradiative decay does not play the dominant role in the excited-state dynamics, because the sum over the quantum yields of IC and ISC is only about 26%. (The room temperature fluorescence quantum yield was determined to be 74%.) Upon a decrease in temperature, the IC quantum yield is reduced as vibrational fluctuations are thermally hindered and the promoter modes of the IC process are less efficiently populated. ISC on the other hand stemming

from a purely electronic coupling is less affected by decreasing temperature.³³ Based on these considerations our experimental results can be understood as the balanced effect of strongly temperature, that is, fluctuation-dependent IC, and less temperature-dependent ISC.^{16,34}

To evaluate the barrier height in a quantitative way, the functional form given in eq 3 was fitted to the data presented in Figure 5. In eq 3, the dependence of the emission lifetime $\tau(T)$ on the temperature and the energy barrier between the bright and a dark excited state is given.³⁵ E_a refers to the activation energy needed for barrier crossing, A is the Arrhenius factor, and $\sum k$ represents the sum over all temperature-independent rates. The constant C accounts for the high-temperature offset of the temperature-dependent data. Following this approach, a barrier height of 36.5 kJ/mol for IC is obtained. The height of this barrier is a good explanation for the high fluorescence quantum yield of about 74%, because nonradiative deactivation directly to the ground state seems to be only a weak effect and the remaining about 26% have a significant contribution of ISC.³⁴

Conclusion

This contribution presents the direct observation of ultrafast excited-state planarization for a conjugated terpyridine system on the example of 4'-4-((2,5-bis(octyloxy)-4-styrylphenyl)ethynyl)phenyl)-2,2':6',2''-terpyridine. Such motion has already been identified to have a strong influence on the excited-state dynamics. However, previously it was not investigated in detail on a model system by tuning solvent parameters such as polarity, viscosity and temperature. The solvent-dependent excited-state processes in the conjugated monoterpyridine derivative were investigated by femtosecond time-resolved absorption and nanosecond time-resolved emission spectroscopy. We report the observation of a 10–100 ps kinetic component, the actual rate of which is strongly solvent-viscosity dependent. Its viscosity dependence, that is, increased rate with decreasing viscosity, indicates that major structural rearrangements are associated with this component. Furthermore, the linear dependence of τ on the solvent viscosity indicates that the excited-state planarization occurs barrierless. The spectral amplitudes of this component do not vary significantly with the polarity of the environment and give no evidence for the contribution of any intramolecular charge-transfer state, which has been speculated to play a role in the excited-state photochemistry of conjugated terpyridine systems. Upon barrierless excited-state planarization a relaxed and emissive excited-state geometry is formed, the emission lifetime of which is found to increase with decreasing temperature. The underlying radiative decay competes with nonradiative processes such as internal conversion back to the ground state and intersystem crossing. Internal conversion, however, plays a minor role only, because this process was found to be thermally activated and to occur over a 36 kJ/mol barrier. However, the crossing of the barrier is not associated with large-scale structural rearrangement of the solute but rather due to thermally activated structural fluctuations.

We expect the direct observation of ultrafast photoinduced planarization in a conjugated terpyridine model system and its detailed dependence on solvent parameters such as viscosity and polarity might impact the design of terpyridine-based polymers with tailored electro-optical properties. Such polymers might find a broad range of applications in artificial light harvesting, polymer solar cells, and organic light-emitting diodes.

Acknowledgment. Financial support of the Fonds der Chemischen Industrie, the Dutch Polymer Institute, the Nederlandse Organisatie voor Wetenschappelijk Onderzoek (VICI award for U.S.S.) and the Thüringer Ministerium für Bildung, Wissenschaft und Kultur (Grant No. B 514-09049, PhotoMIC) for this work is highly acknowledged. We thank Dr. Denis Akimov for technical assistance with the experimental setup and Dr. Michael Schmitt and Prof. Dr. Ulrich-Walter Grummt for helpful discussions.

Supporting Information Available: Additional data and figures. This material is available free of charge via the Internet at <http://pubs.acs.org>.

References and Notes

- (1) (a) Rau, S.; Walther, D.; Vos, J. G. *Dalton Trans.* **2007**, 9, 915–919, and references cited therein. (b) Lewis, N. S.; Nocera, D. G. *Proc. Natl. Acad. Sci. U.S.A.* **2006**, *103*, 15729–15735, and references cited therein.
- (2) (a) Thompson, B. C.; Frechet, J. M. J. *Angew. Chem., Int. Ed.* **2008**, *120*, 62–82. (b) Duprez, V.; Biancardo, M.; Spanggaard, H.; Krebs, F. C. *Macromolecules* **2005**, *38*, 10436–10448. (c) O'Regan, B.; Grätzel, M. *Nature* **1991**, *353*, 737–739. (d) McNamara, W. R.; Snoberger, R. C.; Li, G.; Schleicher, J. M.; Cady, C. W.; Poyatos, M.; Schmittenmaer, C. A.; Crabtree, R. H.; Brudvig, G. W.; Batista, V. S. *J. Am. Chem. Soc.* **2008**, *130*, 14329–14338.
- (3) Scandola, F.; Chiorboli, C.; Prodi, A.; Iengo, E.; Alessio, E. *Coord. Chem. Rev.* **2006**, *250*, 1471–1496.
- (4) Hoppe, H.; Sacrittici, N. S. *Adv. Polym. Sci.* **2008**, *214*, 1–86.
- (5) Pefkianakis, E. K.; Tzanetos, N. T.; Chochos, C. L.; Andreapoulou, A. K.; Kallitsis, J. K. *J. Polym. Sci., Part A: Polym. Chem.* **2009**, *47*, 1939–1952.
- (6) (a) Schubert, U. S.; Hofmeier, H.; Newkome, G. R. *Modern Terpyridine Chemistry*; VCH-Wiley: Weinheim, 2006. (b) Andres, P. R.; Schubert, U. S. *Adv. Mater.* **2004**, *16*, 1043–1068.
- (7) (a) Medlycott, E. A.; Hanan, G. S. *Coord. Chem. Rev.* **2006**, *250*, 1763–1782. (b) Campagna, S.; Puntoriero, F.; Nastasi, F.; Bergamini, G.; Balzani, V. *Top. Curr. Chem.* **2007**, *280*, 117–214. (c) Tschierlei, S.; Presselt, M.; Kuhnt, C.; Yartsev, A.; Pascher, T.; Sundström, V.; Karnahl, M.; Schwalbe, M.; Schäfer, B.; Rau, S.; Schmitt, M.; Dietzek, B.; Popp, J. *Chem.—Eur. J.* **2009**, *15*, 7678–7688. (d) Siebert, R.; Winter, A.; Dietzek, B.; Schubert, U. S.; Popp, J. *Macromol. Rapid Commun.* **2010**, DOI: 10.1002/marc.200900894.
- (8) Barbieri, A.; Ventura, B.; Barigelletti, F.; De Nicola, A.; Quesada, M.; Ziessel, R. *Inorg. Chem.* **2004**, *43*, 7359–7369.
- (9) Medlycott, E. A.; Hanan, G. S. *Chem. Soc. Rev.* **2005**, *34*, 133–142.
- (10) Maestri, M.; Armaroli, N.; Balzani, V.; Constable, E. C.; Cargill Thompson, A. M. W. *Inorg. Chem.* **1995**, *34*, 2759–2767.
- (11) (a) Abrahamsson, M.; Jäger, M.; Österman, T.; Eriksson, L.; Persson, P.; Becker, H. C.; Johansson, O.; Hammarström, L. *J. Am. Chem. Soc.* **2006**, *128*, 12616–12617. (b) Schulze, B.; Friebe, C.; Hager, M. D.; Winter, A.; Hoogenboom, R.; Görls, H.; Schubert, U. S. *Dalton Trans.* **2009**, 787–794.
- (12) Wang, X. Y.; Guerso, A.; Tunuguntla, H.; Schmehl, R. H. *Res. Chem. Int.* **2007**, *33*, 63–77.
- (13) (a) Egbe, D. A. M.; Carbonnier, B.; Birkner, E.; Grummt, U. W. *Prog. Polym. Sci.* **2009**, *34*, 1023–1067. (b) Grimsdale, A. C.; Chan, K. L.; Martin, R. E.; Jokisz, P. G.; Holmes, A. B. *Chem. Rev.* **2009**, *109*, 897–1091.
- (14) (a) Winter, A.; Friebe, C.; Hager, M. D.; Schubert, U. S. *Macromol. Rapid Commun.* **2008**, *29*, 1679–1686. (b) Winter, A.; Friebe, C.; Chiper, M.; Hager, M. D.; Schubert, U. S. *J. Polym. Sci., Part A: Polym. Chem.* **2009**, *47*, 4083–4098. (c) Chen, Y. Y.; Tao, Y. T.; Lin, H. C. *Macromolecules* **2006**, *39*, 8559–8566.
- (15) (a) Winter, A.; Friebe, C.; Chiper, M.; Schubert, U. S.; Presselt, M.; Dietzek, B.; Schmitt, M.; Popp, J. *ChemPhysChem* **2009**, *10*, 787–798. (b) Presselt, M.; Dietzek, B.; Schmitt, M.; Popp, J.; Winter, A.; Chiper, M.; Friebe, C.; Schubert, U. S. *J. Phys. Chem. C* **2008**, *112*, 18651–18660.
- (16) Siebert, R.; Akimov, D.; Schmitt, M.; Winter, A.; Schubert, U. S.; Dietzek, B.; Popp, J. *ChemPhysChem* **2009**, *10*, 910–919.
- (17) (a) Damrauer, N. H.; Boussie, T. R.; Devenney, M.; McCusker, J. K. *J. Am. Chem. Soc.* **1997**, *119*, 8253–8268. (b) Damrauer, N. H.; McCusker, J. K. *J. Phys. Chem. A* **1999**, *103*, 8440–8446. (c) Lainé, P. P.; Campagna, S.; Loiseau, F. *Coord. Chem. Rev.* **2008**, *252*, 2552–2571. (d) Lainé, P. P.; Bedioui, F.; Loiseau, F.; Chiorboli, C.; Campagna, S. *J. Am. Chem. Soc.* **2006**, *128*, 7510–7521.
- (18) (a) Polivka, T.; Sundström, V. *Chem. Rev.* **2004**, *104*, 2021–2071. (b) Zigmantas, D.; Hiller, R. G.; Yartsev, A.; Sundström, V.; Polivka, T. *J. Phys. Chem. B* **2003**, *107*, 5339–5348. (c) Zigmantas, D.; Hiller, R. G.; Sharples, F. P.; Frank, H. A.; Sundström, V.; Polivka, T. *Phys. Chem. Chem. Phys.* **2004**, *6*, 3009–3016.
- (19) (a) Dietzek, B.; Tschierlei, S.; Herman, G.; Yartsev, A.; Pascher, T.; Sundström, V.; Schmitt, M.; Popp, J. *ChemPhysChem* **2009**, *10*, 144–150. (b) Dietzek, B.; Kiefer, W.; Yartsev, A.; Sundström, V.; Schellenberg, P.; Grigavicius, P.; Herman, G.; Popp, J.; Schmitt, M. *ChemPhysChem* **2006**, *7*, 1727–1733.
- (20) Winter, A.; Friebe, C.; Hager, M. D.; Schubert, U. S. *Eur. J. Org. Chem.* **2009**, 801–809.
- (21) Lippert, E. Z. *Elektrochem.* **1957**, *61*, 962–975.
- (22) (a) Nad, S.; Pal, H. *J. Phys. Chem. A* **2001**, *105*, 1097–1106. (b) Grummt, U. W.; Weiss, D.; Birkner, E.; Beckert, R. *J. Phys. Chem. A* **2007**, *111*, 1104–1110. (c) Fery-Forgues, S.; Fayet, J. P.; Lopez, A. J. *Photochem. Photobiol. A* **1993**, *70*, 229–243.
- (23) (a) Chen, X.; Zhou, Q.; Cheng, Y.; Geng, Y.; Ma, D.; Xie, Z.; Wang, L. *J. Lumin.* **2007**, *126*, 81–90. (b) Wang, X. Y.; Guerso, A.; Schmehl, R. H. *Chem. Commun.* **2002**, 2344–2345. (c) Leroy, S.; Soujanya, T.; Fages, F. *Tetrahedron Lett.* **2001**, *42*, 1665–1667. (d) Tessore, F.; Roberto, D.; Ugo, R.; Pizzotti, M. *Inorg. Chem.* **2005**, *44*, 8967–8978.
- (24) Dietzek, B.; Kiefer, W.; Hermann, G.; Popp, J.; Schmitt, M. *J. Phys. Chem. B* **2006**, *110*, 4399–4406.
- (25) Akesson, E.; Bergström, H.; Sundström, V.; Gillbro, T. *Chem. Phys. Lett.* **1986**, *126*, 385–393.
- (26) (a) Bagchi, B.; Fleming, G. R. *J. Phys. Chem.* **1990**, *94*, 9–20. (b) Bagchi, B.; Fleming, G. R.; Oxtoby, D. W. *J. Chem. Phys.* **1983**, *78*, 7375–7385.
- (27) (a) Dietzek, B.; Tarnovsky, A. N.; Yartsev, A. *Chem. Phys.* **2009**, *357*, 54–62. (b) Dietzek, B.; Christensson, N.; Pascher, T.; Pullerits, T.; Yartsev, A. *J. Phys. Chem. B* **2007**, *111*, 5396–5404. (c) Akers, W.; Haidekker, M. A. *Trans. ASME* **2004**, *126*, 340–345.
- (28) (a) Todd, D. C.; Fleming, G. R. *J. Chem. Phys.* **1993**, *98*, 269–279. (b) Aberg, U.; Sundström, V. *Chem. Phys. Lett.* **1991**, *185*, 461–467.
- (29) (a) Di Paolo, R. E.; Seixas de Melo, J.; Pina, J.; Burrows, H. D.; Morgado, J.; Macanita, A. L. *ChemPhysChem* **2007**, *8*, 2657–2664. (b) Di Paolo, R. E.; Burrows, H. D.; Morgado, J.; Macanita, A. L. *ChemPhysChem* **2009**, *10*, 448–454.
- (30) Sluch, M. I.; Godt, A.; Bunz, U. H.; Berg, M. A. *J. Am. Chem. Soc.* **2001**, *123*, 6447–6448.
- (31) (a) Horng, M. L.; Gardecki, J. A.; Papazyan, A.; Maroncelli, M. *J. Phys. Chem.* **1995**, *99*, 17311–17337. (b) Horng, M. L.; Gardecki, J. A.; Maroncelli, M. *J. Phys. Chem. A* **1997**, *101*, 1030–1047.
- (32) Aleman, E. A.; Shreiner, C. D.; Rajesh, C. S.; Smith, T.; Garrison, S. A.; Modarelli, D. A. *Dalton Trans.* **2009**, 6562–6577.
- (33) (a) Larson, E. J.; Johnson, C. K. *J. Phys. Chem. B* **1999**, *103*, 10917–10923. (b) Mac, M.; Kwiatkowski, P.; Pischel, U. *Chem. Phys. Lett.* **2002**, *357*, 440–449.
- (34) (a) Burrows, H. D.; Seixas de Melo, J.; Serpa, C.; Arnaut, L. G.; Miguel, M. G.; Monkman, A. P.; Hamblett, I.; Navaratnam, S. *Chem. Phys.* **2002**, *285*, 3–11. (b) Pina, J.; Seixas, M.; Burrows, H. D.; Galbrecht, F.; Bilge, A.; Kudla, C. J.; Scherf, U. *J. Phys. Chem. B* **2008**, *112*, 1104–1111.
- (35) (a) Lewis, F. D.; Zuho, X. *J. Am. Chem. Soc.* **2003**, *125*, 8806–8813. (b) Yang, J. S.; Liao, K. L.; Hwang, C. Y.; Wang, C. M. *J. Phys. Chem. A* **2006**, *110*, 8003–8010.

JP100313X